

**SG2PS (STRUCTURAL GEOLOGY TO POSTSCRIPT CONVERTER) – A
GRAPHICAL SOLUTION FOR BRITTLE STRUCTURAL DATA
EVALUATION AND PALEOSTRESS CALCULATION**

Ágoston SASVÁRI^{1}, Ali BAHAREV²*

¹ Structural geologist, Llandudno, North Wales, United Kingdom

² Chemical engineer and software developer, Vienna, Austria

* Corresponding author.

telephone: +44-7585-77-0760;

email address: sasvariagoston@yahoo.com;

present address: 73 Hill View Road, Llanrhos,
LL301SL, North Wales, United Kingdom.

ABSTRACT

The aim of this work was to create an open source cross platform application to process brittle structural geological data with seven paleostress inversion algorithms published by different authors and formerly not available within a single desktop application. The tool facilitates separate processing and plotting of different localities, data types and user made groups, using the same single input file. Simplified data input is supported, requiring as small amount of data as possible. Data rotation to correct for bedding tilting, rotation with paleomagnetic declination and *k*-means clustering are available. RUP and ANG stress estimators calculation and visualisation, resolved shear direction display and Mohr circle stress visualisation are available.

RGB-coloured vector graphical outputs are automatically generated in Encapsulated PostScript and Portable Document Format. Stereographical displays on great circle or pole point plot, equal area or equal angle net and upper or lower hemisphere projections are implemented. Rose plots displaying dip direction or strike, with dip angle distribution of the input data set are available. This tool is ideal for preliminary data interpretation on the field (quick processing and visualization in seconds); the implemented methods can be regularly used in the daily academic and industrial work as well.

The authors' goal was to create an open source and self-contained desktop application that does not require any additional third party framework (such as .NET) or the Java Virtual Machine. The software has a clear and highly modular structure enabling good code portability, easy maintainability, reusability and extensibility. A Windows installer is publicly available and the program is also fully functional on Linux. The Mac OS X port should be feasible with minimal effort. The install file with test and demo data sets, detailed manual, and links to the GitHub repositories are available on the regularly updated website www.sg2ps.eu.

KEY WORDS

Paleostress inversion; Angelier method; graphical user interface; RUP; slickenside; cluster analysis

1 INTRODUCTION

Paleostress inversion methodologies – based on different assumptions and using different calculation procedure – were published by several authors (e.g. [Turner 1953](#),

Spang 1972, Carey and Brunier 1974, Angelier and Mechler 1977, Angelier 1975, 1979, 1984, 1990, Angelier and Goguel 1979, Etchecopar et al. 1981, Gephart and Forsyth 1984, Michael 1984, Reches 1987, Huang 1988, Will and Powell 1991, Nemčok and Lisle 1995, Yin and Ranalli 1995, Fry 1999, Nemčok et al. 1999, Orife et al. 2002 and Tobore and Lisle 2003). Based on this knowledge, some authors developed and published their own computer based solutions either for brittle structural data processing, or for paleostress inversion (e.g. Lisle 1988, Gephart 1990, Hardcastle and Hills 1991, Krejci and Richter 1991, Taboada et al. 1991, Sperner et al. 1993, Sperner and Ratschbacher 1994, Shorrock and Lisle 1998, Lisle and Orife 2002, Shan et al. 2004, Pascal 2004 and Mostafa 2005). Using theoretical background and previous explorers' software experience, some authors and companies developed complete computer based implementations or web applications for brittle structural data processing (e.g. Yamaji 2001, Tomita and Yamaji 2004, Faille 2010, GEOrient 2011, Openstereo 2011, Cardozo and Allmendinger 2013 and their code OSXStereonet 2012, Fabric 2012, Orient 2012, Dips 2013, FaultKin 2013, RockWare StereoStat 2013, RockWare SpheriStat 2013, Stereonet 2013 and Stereonet Web Application 2013) and for paleostress calculation (e.g. TECTOR 1994, TECTOR 2000, Yamaji 2000, Ortner et al. 2002, Delvaux and Sperner 2003 and their code Win-Tensor 2012, Žalohar and Vrabec 2007, FSA 2013 and MyFault 2013) with own web page, documentation and Grapical User Interface (GUI) ready for daily use. An extensive comparison of these applications is given in Table 1.

Based on Table 1, the main goal of the authors' work was to create a novel *free* and *open source* solution for brittle structural data processing with a *Grapical User Interface* (GUI). Easy-to-use and regularly updated *webpage* with *test data sets* and

references, *comprehensive manual*, *software history* as well as the *documentation* of the applied methodologies have key importance in serving the user's needs.

Simplified data input (possibility to leave cells empty and enter as less data as required to the processing) reduces time requirements of data evaluation. Cross platform data formats, e.g. *tab separated text file* (Shafranovich 2005) as input and vector graphical *Encapsulated PostScript* (EPS, [Adobe Developer Support, 1992](#)) or *Portable Document Format* (PDF, [Adobe System Incorporated, 2006](#)) as output allows flexible and user friendly data handling.

Ability of data *separation* into user defined subsets, *k-means clustering* of input data set, *average bedding calculation* and automatic *data rotation to correct for bedding tilting and/or paleomagnetic declination* (referred to as *BN rotation* from now on) offers a wide range combination of data evaluation methodologies.

Large number of implemented *paleostress inversion methodologies* ([Turner 1953](#), [Spang 1972](#), [Michael 1984](#), [Angelier 1990](#), [Fry 1999](#), [Shan et al. 2004](#), and [Mostafa 2005](#), for comparison see [Appendix 1](#)), reduced stress tensor calculation (after both [Bishop 1966](#) and [Delvaux et al. 1997](#)), as well as RUP and ANG estimators calculation ([Angelier 1990](#)) enlarges reliability and control of paleostress inversion.

2 HIGH-LEVEL PROGRAM OVERVIEW

SG2PS software package is composed of three main parts: the *graphical user interface* ('sg2ps_GUI.exe') controls the work of the *console application*

(‘sg2ps.exe’). Following the data evaluation, the *converter* (‘ps2pdf.exe’) optionally calls the GPL Ghostscript interpreter to perform the PostScript to PDF conversion.

Great care was taken to implement the program in a cross-platform manner.

Currently, a Windows installer is publicly available. The program is also fully functional on the Linux operating system since significant part of the development was carried out on Linux. The Mac OS X port should be feasible with minimal effort and it is among the authors’ plans; unfortunately the authors do not have access to this operating system.

The program is fully functional if the user can view *Portable Document Format* files and edit spreadsheets documents (for example Microsoft Excel). System administrator rights are not required for the installation; the program can be installed into any directory, even on a USB stick.

2.1 EXECUTABLES

2.1.1 GRAPHICAL USER INTERFACE

The *graphical user interface* (Figure 1) gives an interactive platform to create new input and coordinate files, as well as to select or manipulate existing ones (see Figure 1A). New empty or existing files can be imported into the default spreadsheet editor to give an easy handling possibility for data input. The project status panel (Figure 1B) shows the project name and path, as well as the existence of the *input data file*, *settings* and *coordinate files* (see Section 2.2). If *user defined* project evaluation settings are available (see Section 2.2 and Section 4), they are displayed on the drop-down lists; otherwise hard-coded program defaults are shown (see Figure 1C). If a

change in processing or display parameters is required, it is possible to do here in an interactive way. Hitting or “Run” button (Figure 1D) starts the data processing with the user-defined settings. The status bar below the “Run” button (Figure 1E) displays the progress of the conversion from *Encapsulated PostScript* to *Portable Document Format* (see later); the name of the actual file being processed is shown.

2.1.2 CONSOLE APPLICATION

The *console application* processes the input files according to the settings made on the graphical user interface (Figure 1C). The console application performs the actual data processing, creates a directory structure and writes the results (see Section 2.4) into the appropriate files. A detailed log, shown on the standard output by default, informs the user about general information, settings, input file error checking steps, results of pre-processing and processing, export status and elapsed time (see Sections 2.3 and 2.4).

2.1.3 CONVERTER

The console application writes the graphical output in *Encapsulated PostScript* format (see Section 2.4). Applications for viewing files in *Portable Document Format* are ubiquitous, hence converting the result EPS files into PDF format proved to be useful. The *converter* ‘ps2pdf.exe’ is a tiny wrapper application calling the GPL Ghostscript interpreter to perform the actual EPS to PDF conversion. Obviously, the converter is run after the data processing. It is optional whether the original EPS files are kept or deleted after the conversion.

2.1.4 PROGRAM DESIGN OVERVIEW

The console application and the GUI are efficiently decoupled from each other: as long as the console application does not break its command line interface, the console application can be updated independently from the GUI and vice-versa. The console application is written in standard C++, hence its code is highly portable. The GUI is inherently dependent on the user's desktop; all the operations that cannot be done in standard C++ are performed by the GUI. For example, file systems paths are both platform and locale dependent, and cannot be handled in standard C++ yet. The GUI is based on Qt, a C++ toolkit for cross-platform application development. Decoupling the responsibilities in this way (*i.e.* platform and locale dependent operations vs. data processing and computations) reduced greatly the code complexity of both applications.

The GUI delegates the graphical tasks to the user's desktop applications: The graphical data input is handled by the user's default spreadsheet editor, the PDF display is performed with the default PDF viewer, etc. If the default application is not appropriate for some reason, it is easy to re-configure the GUI to invoke a user-specified desktop application instead. This sort of delegation of the graphical data input and display tasks saves a tremendous implementation and maintenance work for the authors.

Finally, the GUI is separated from the GPL Postscript interpreter through a tiny wrapper application, see subsection 2.1.3. This accounts for the variations in the ways the different platforms invoke the PostScript interpreter.

2.2 INPUT FILES

The entire data processing is based on the concept of *project*. To process a *data set*, at least one *input data file* has to exist in the *working directory* whose name will be used as *project name* (see [Figure 1B](#)). The following three files – with the *same name* but *different extension* – are used during the data processing: 1) *input data file* (obligatory) which is a tab separated text file with ‘rgf’ extension (for the further details see [the manual on the www.sg2ps.eu /manual website](http://www.sg2ps.eu/manual)), a 2) *coordinate file* (optional) with locality coordinates and formation names with ‘xy’ extension (see [the manual on the www.sg2ps.eu /manual website](http://www.sg2ps.eu/manual)) and a 3) *settings file* (optional) with ‘set’ extension (see [Section 4](#)).

If the coordinate file is correct, its content is merged with the input file content: *these* final coordinates and formation names are used during processing and exporting. If the coordinate file is missing or the file structure is incorrect, it is not processed (see [Section 2.3.1](#)).

The user can modify the processing and display settings (see [Section 4](#)) on the interactive menu; after modifications, the settings file is saved automatically and the input file is ready for processing.

2.3 DATA PROCESSING

If the evaluation is started by hitting the Run button, the GUI calls the console application to process the input data files. The data processing is composed of several different steps in the following order. *Input data file validation* is executed first to ensure processed data are in agreement with [the input file requirements](#). This step is followed by the *quality check of the coordinate file*. After *completion* of input data

set, *pre-processing* and *processing* (Section 2.3.3) is performed, before data sets and subsets are exported into text files and vector graphic files (Section 2.4).

2.3.1 INPUT FORMAT CHECK

In the first step, the *input data file* validation is carried out to avoid processing of incorrect data sets. During this step, both the input data file and the coordinate file are checked column by column. If the input data file does not fit the hard coded standards, the processing terminates and an error message informs the user about the issue. If the input data file content is correct, it will be imported and an *input data set* is generated.

If the coordinate file content conflicts with the standards, the processing terminates, and an error message informs the user about the issue; otherwise, the coordinate file will be used.

2.3.2 PRE-PROCESSING

The pre-processing phase is carried out in the following order on the already checked input *data set*. First step is *data base completion*: filling of empty database records with data in agreement to the philosophy as described in the manual on the www.sg2ps.eu/manual website. *Small artificial random errors* are generated to avoid division by zero when eigenvectors and eigenvalues are calculated for centric data set. *Striae misfit calculation* is carried out for slickensides entered in lineation format in the following way (no misfit correction is required for pitch data). According to the usual field experience (when the slip line measurement is more difficult than the fault plane measurement), it is assumed that the fault plane measurement was reliable and the slip line measurement is corrected. This correction is possible in the following

way: Either assuming the measured slip line azimuth is correct and the *plunge* has to be modified, or accept the plunge as correct and change the *azimuth*. In the recent version of the software, correction resulting in the smallest angular change is applied.

If it is requested by the user, *k-means clustering* is carried out for the input data set (see [Section 4](#)). *Compression, extension and intermediate axes* are calculated for each slickenside data, if [Turner \(1953\)](#) paleostress inversion methodology is selected.

In the next step, *data averages* are computed for each data types location by location, except ‘lithology’, ‘s-c’ and ‘striae’ data; *singularities cross check* for each data set is needed prior the average calculation. During the used regression (see later, [Bingham 1964, 1974](#)), a directional tensor is calculated (see [Appendix 1](#)). If the tensor is singular or nearly singular, no data set average is calculated. Average bedding data and paleomagnetic declination (if available and required, see [Section 4](#)) is used to *BN rotate* all measurements; a second data set is generated containing the BN rotated data. For more than two records with the same data type, regression after [Bingham \(1964, 1974\)](#) is carried out to find the maximum weight point orientation of the input data set.

2.3.3 PROCESSING AND OUTPUT

The general processing philosophy is to generate data *subsets* – for both *original* and *BN corrected sets* – with the same locality, data type and data group (if preferred, see [Section 4](#)), to process and export these subsets one by one.

The first step is the *paleostress calculation* for slickenside data, and *weight point statistics* calculation for fracture data subsets (see [Appendix 1](#)). Processed subsets are *exported* into text files to be ready for further evaluation.

Average data – calculated during the pre-processing (see [Section 2.3.2](#)) – are exported in the same file for further use in GIS systems. The last phase of output is *Portable Document Format* creation and optional removal of the original *Encapsulated PostScript* files.

2.4 OUTPUT

The output files are placed under the specific directory structure detailed below. To avoid accidentally overwriting results from a previous run, a unique *project folder* is created in the *working directory* for each run.

Output files are stored in five different subfolders of the project folder. The ‘1_original’ folder contains the copy of the original *input, coordinate* and *setting files* with no modifications as backup and the processing *log* generated by the console application. The ‘2_completed’ folder contains the *completed version* of the original input file with no empty records ([Section 2.2](#)). The ‘3_average’ folder has one file for the average data, calculated for each localities and for each different data types. Both the ‘4_rgf_separated’ and the ‘5_ps_separated’ folders have different subfolders named after the existing data types found in the input file. These subfolders are containing completed input files and graphical results (*Encapsulated PostScript* and/or *Portable Document Format* files), separated by data points and data types. Both the *original* and *BN rotated* sets are exported here.

3. THE FINAL GRAPHICAL OUTPUT

The final graphical product (see [Figure 2](#)) is an A3-size sheet in *Encapsulated PostScript* and/or *Portable Document Format*, built up by an *upper* and a *lower* panel displaying the *observed* ([Figure 2A](#)) and *BN rotated* data ([Figure 2B](#)) on stereonet and rose diagrams. At the left upper corner ([Figure 2C](#)), *data locality*, *data type* and *group name* are indicated. *Number* of displayed data with the *average bedding* used for BN rotation, as well as the *rotation methodology* are shown on the upper left corner of the stereonet ([Figure 2D](#)). *Plot type*, *projection* and *hemisphere* are displayed on the lower left corner of the stereonet ([Figure 2E](#)).

If slickenside data are processed, paleostress inversion result is presented below the stereonet on the right hand side (see [Figure 2F](#)): paleostress inversion *methodology*, stress axes *directions*, reduced *stress tensors* value after [Bishop \(1966\)](#) and [Delvaux et al. \(1997\)](#) as well as the *stress regime* according to [Delvaux et al. \(1997\)](#). Red, green and blue diamonds ([Figure 2G](#)) show *maximum*, *intermediate* and *minimum* stress axes, black and white arrows show the *maximum* and *minimum horizontal stress axes*. If fractures with no striation are processed, directional analysis results – density ellipsoid axis directions and axes length – are displayed. Red, green and blue diamonds show *maximum*, *intermediate* and *minimum* weight axis orientation.

Rainbow-coloured bar on the right hand side of the stereonet ([Figure 2H](#)) shows the possible stress regimes from radial extensive (black) to radial compressive (red), and thick white line indicates the current stress regime after paleostress inversion. The RUP bar ([Figure 2I](#), not available if paleostress inversion is carried out after [Turner](#)

1953, Spang 1972 and Michael 1984) displays the *relative epsilon* value (theoretical / resolved shear stress vector length) from 0 to maximum RUP value after Angelier (1990). Thickness of gray bars in the background shows *the relative interval density* of RUP values. ANG bar (Figure 2J) shows the *angular misfit* between the measured and resolved stress directions from 0 to the maximum ANG value. Thickness of gray bars in the background shows the interval density of ANG values.

Equal bin size rose plots show directional density of the evaluated data set (dip or strike of the input data set according to the user's choice); symmetric and asymmetric plots with different bin size are available. Main circular rose diagram (Figure 2K) is designed for horizontal (strike or dip direction) distribution; small quadrant plot (Figure 2L) shows vertical (dip angle or plunge) directional statistics. In the case of planes and lineations, green pie charts show relative density of data dip direction. If slickensides or s-c planes are evaluated, green pies show relative density of striated planes or s planes; blue transparent pies are displaying relative density of slickenside slip direction or c plane dip direction.

Mohr circles (Figure 2M) show the stress status as well as normalized normal and shear stress values for each evaluated data; Mohr circle colour refers to the stress regime.

4 SETTINGS AND VISUALIZATION

A variety of display, processing and visualization options are available. If a settings file (see Section 2.2) is used, the options are displayed on the *graphical user interface*. If no settings file is used, the default hard coded options are used.

Before data processing, the user can define the processing and display methodologies by choosing from a pre-defined list of options. The user's choice is then saved into a *settings file* (and also stored in the result project directory, see [Section 2.4](#)).

Before data evaluation, the user can modify the display and processing preferences. *Dip direction or right hand rule* data convention, *great circle or pole point* display ([Hoeppener 1955](#)), *equal area or equal angle* projections ([Figure 3A and 3B](#)) on *upper or lower* hemisphere plots are available. If average bedding geometry was calculated or paleomagnetic declinations are available, it is possible to rotate these observations to correct for bedding tilting for each data point, rotate them with the *paleomagnetic declination*, or do *both* corrections in the same time (see [Figure 4A, 4B, 4C and 4D](#)).

In the course of processing, it is possible to use user-defined groups on two different ways. The first possibility is to *take groups into account*; in this case all data will be separated by locality, data type and groups, and coloured by black on the output files ([Figure 5A](#)). On the other hand, if groups are *not* taken into agreement, the processing will be done by locality and data type, and the final stereonet will be coloured by the different groups ([Figure 5B](#)). *K-means clustering* (first [Steinhaus 1957](#); see e.g. [MacQueen 1967](#)) of the input data set could be carried out: either the user can define cluster numbers, or the software can determine the best fitting cluster number ([Figure 6](#)).

For slickenside processing, *paleostress inversion* can be carried out using the methodology of Turner (1953), Spang (1972), Michael (1984), Angelier (1990), Fry (1999), Shan et al. (2004), and Mostafa (2005) as shown in Figures 7A – 7G and shortly described in Appendix 1. *Virtual symmetrical data set* could be used to artificially produce forced Andersonian (Anderson 1942) stress state. During this processing step, *central symmetrical copy* of the original input data subset, plus the input data set itself are used for paleostress calculation (see Figures 8A and 8B). *Resolved shear direction* display shows theoretical slip direction on each striated planes in the calculated paleostress state.

Turner's (1953) and Spang's (1972) methodologies need *maximum stress direction to slickenside direction angle*: this is the angle of the maximum horizontal stress direction to the slip movement (slickenside) direction. According to the general rock mechanical knowledge (see e.g. Handin 1966), this value is usually around 30 degrees; values between 10 and 80 degrees can be set in the software. For fractures, a *directional weight point statistics* (Bingham 1964, 1974) can be selected by the user.

On the final plots, rose diagrams of the input data set dip *directions* or *strikes* with *symmetric* or *asymmetric* display, using 2.5, 5, 10 or 22.5 degree bin sizes are available (Figures 9A – 9D). All data should be *labelled* with its independent ID; *line width* on these plots has a range of 0.1 – 1.0 points. According to the user's choice *RGB coloured* or *greyscale* output is possible.

5 CONCLUSIONS

A user friendly, easy to use open source cross platform application was developed to process brittle structural geological data with various paleostress inversion algorithms published by different authors and formerly not available within a single application. Simplified data input option, automatic data rotation to correct for bedding tilting, as well as input data clustering options were developed. RGB and greyscale vector output is produced by the software according to the EPS and PDF standards. The software has a clear and highly modular structure enabling good code portability and easy maintainability. The application is self-contained: the user does not have to install any additional third party framework; the program can be installed even on a USB stick.

At this stage, SG2PS can be an effective data processing tool for both the academic and the industrial sector. New separation tools for heterogeneous brittle structural data (clustering after paleostress inversion in RUP and/or ANG parameters based on [Angelier's 1990](#) idea) are being currently implemented together with different contouring options and an automatic bedding tilting versus brittle deformation chronology module. Hopefully this software can be a good 'case study' to develop a final graphical, GIS-based interactive solution for comprehensive brittle deformation data processing.

6 *ACKNOWLEDGEMENT*

The first author started to work on the early version of this program at MOL Plc. (Hungary), where his managers and colleagues – Gizella Bagoly-Árgyelán and László Csontos – were so kind to contribute and help the development. Agust Gudmundsson, Françoise Bergerat and Bernard Célérier gave help to understand the fine details of Angelier's paleostress inversion methodology. Useful comments of Jef Caers

regarding the paper structure are really appreciated. Special thanks for Christophe Pascal and Damian Delvaux for their effort reviewing the manuscript.

APPENDIX 1: practical overview of the implemented paleostress inversion methodologies

1A Bingham (1964, 1974)

This methodology is used to visualize directional distribution of fractures calculating their three dimensional density ellipsoid using regression.

- Generate unit vectors n , e and u parallel to the coordinate axes;
- Calculate the sum E of the following directional tensors E_i for each i^{th} slickenside using plane normal N_i (ang is the angle between two vectors):

$$E_i = \begin{bmatrix} \varepsilon_{11} & \varepsilon_{12} & \varepsilon_{13} \\ \varepsilon_{12} & \varepsilon_{22} & \varepsilon_{23} \\ \varepsilon_{13} & \varepsilon_{23} & \varepsilon_{33} \end{bmatrix}$$

where

$$\begin{aligned} \varepsilon_{11} &= \text{ang}(N_i, e) \text{ang}(N_i, e), \\ \varepsilon_{12} &= \text{ang}(N_i, e) \text{ang}(N_i, n), \\ \varepsilon_{13} &= \text{ang}(N_i, e) \text{ang}(N_i, u), \\ \varepsilon_{22} &= \text{ang}(N_i, n) \text{ang}(N_i, n), \\ \varepsilon_{23} &= \text{ang}(N_i, n) \text{ang}(N_i, u), \\ \varepsilon_{33} &= \text{ang}(N_i, u) \text{ang}(N_i, u). \end{aligned}$$

- Eigenvectors of tensor E are the maximum, minimum and intermediate axes of the directional distribution ellipsoid; eigenvalues equal to the axes length.

1B Spang (1972)

This is a simple linear regression with *a priori* assumption on the angle α between the slip vector ($SV_i = [SV_X \ SV_Y \ SV_Z]$) and the maximum stress direction.

- Generate unit vectors n , e and u parallel to the coordinate axes;
- Calculate p_i and t_i compressional and tensional directional vectors for each i^{th} slickenside, using the fault plane normal vector ($N_i = [N_X \ N_Y \ N_Z]$):

$$p_i = \begin{bmatrix} (90 - \alpha)SV_X - \alpha N_X \\ (90 - \alpha)SV_Y - \alpha N_Y \\ (90 - \alpha)SV_Z - \alpha N_Z \end{bmatrix} \text{ and } t_i = \begin{bmatrix} (90 - \alpha)N_X + \alpha SV_X \\ (90 - \alpha)N_Y + \alpha SV_Y \\ (90 - \alpha)N_Z + \alpha SV_Z \end{bmatrix}$$

- Stress tensor components are calculated in the following way:

$$\sigma_{11} = \text{ang}(p_i, e) \text{ang}(p_i, e) - \text{ang}(t_i, e) \text{ang}(t_i, e)$$

$$\sigma_{12} = \text{ang}(p_i, e) \text{ang}(p_i, n) - \text{ang}(t_i, e) \text{ang}(t_i, n),$$

$$\sigma_{13} = \text{ang}(p_i, e) \text{ang}(p_i, u) - \text{ang}(t_i, e) \text{ang}(t_i, u),$$

$$\sigma_{22} = \text{ang}(p_i, n) \text{ang}(p_i, n) - \text{ang}(t_i, n) \text{ang}(t_i, n),$$

$$\sigma_{23} = \text{ang}(p_i, n) \text{ang}(p_i, u) - \text{ang}(t_i, n) \text{ang}(t_i, u),$$

$$\sigma_{33} = \text{ang}(p_i, u) \text{ang}(p_i, u) - \text{ang}(t_i, u) \text{ang}(t_i, u).$$

1C Turner (1953)

This methodology is a linear regression with the same *a priori* assumption on the angle α as in Spang's (1972) method.

- Generate unit vectors n , e and u parallel to the coordinate axes;
- Calculate pressure (p_i) and tension (t_i) vectors for each i^{th} slickenside in the same way as in the case of Spang's (1972) method;
- Calculate neutral vectors as follows: $n_i = p_i \otimes t_i$ (where \otimes denotes cross product);
- Calculate the sum of the following directional tensors P_i , T_i and N_i :

$$P_i = \begin{bmatrix} \text{ang}(p_i, e) \cdot \text{ang}(p_i, e) & \text{ang}(p_i, e) \cdot \text{ang}(p_i, n) & \text{ang}(p_i, e) \cdot \text{ang}(p_i, u) \\ \text{ang}(p_i, e) \cdot \text{ang}(p_i, n) & \text{ang}(p_i, n) \cdot \text{ang}(p_i, n) & \text{ang}(p_i, n) \cdot \text{ang}(p_i, u) \\ \text{ang}(p_i, e) \cdot \text{ang}(p_i, u) & \text{ang}(p_i, n) \cdot \text{ang}(p_i, u) & \text{ang}(p_i, u) \cdot \text{ang}(p_i, u) \end{bmatrix},$$

$$T_i = \begin{bmatrix} \text{ang}(t_i, e) \cdot \text{ang}(t_i, e) & \text{ang}(t_i, e) \cdot \text{ang}(t_i, n) & \text{ang}(t_i, e) \cdot \text{ang}(t_i, u) \\ \text{ang}(t_i, e) \cdot \text{ang}(t_i, n) & \text{ang}(t_i, n) \cdot \text{ang}(t_i, n) & \text{ang}(t_i, n) \cdot \text{ang}(t_i, u) \\ \text{ang}(t_i, e) \cdot \text{ang}(t_i, u) & \text{ang}(t_i, n) \cdot \text{ang}(t_i, u) & \text{ang}(t_i, u) \cdot \text{ang}(t_i, u) \end{bmatrix}, \text{ and}$$

$$N_i = \begin{bmatrix} \text{ang}(n_i, e) \cdot \text{ang}(n_i, e) & \text{ang}(n_i, e) \cdot \text{ang}(n_i, n) & \text{ang}(n_i, e) \cdot \text{ang}(n_i, u) \\ \text{ang}(n_i, e) \cdot \text{ang}(n_i, n) & \text{ang}(n_i, n) \cdot \text{ang}(n_i, n) & \text{ang}(n_i, n) \cdot \text{ang}(n_i, u) \\ \text{ang}(n_i, e) \cdot \text{ang}(n_i, u) & \text{ang}(n_i, n) \cdot \text{ang}(n_i, u) & \text{ang}(n_i, u) \cdot \text{ang}(n_i, u) \end{bmatrix}$$

- Calculate the eigenvalues ($e_{P1} \geq e_{P2} \geq e_{P3}$, $e_{T1} \geq e_{T2} \geq e_{T3}$, $e_{N1} \geq e_{N2} \geq e_{N3}$) and the referring eigenvectors (E_{P1} , E_{P2} , E_{P3} , E_{T1} , E_{T2} , E_{T3} , E_{N1} , E_{N2} , E_{N3}) for P_i , T_i and N_i tensors, respectively;
- The maximum, intermediate and minimum stress directions will be E_{P1} , E_{N2} , and E_{T3} , respectively; the reduced stress tensor T_r will be:

$$T_r = \begin{bmatrix} \sigma_1 & 0 & 0 \\ 0 & \sigma_2 & 0 \\ 0 & 0 & \sigma_3 \end{bmatrix} = \begin{bmatrix} e_{P1} & 0 & 0 \\ 0 & e_{N2} & 0 \\ 0 & 0 & e_{T3} \end{bmatrix}.$$

1D Fry (1999)

Fry's (1999) methodology is a six dimensional regression to solve Angelier's (1979) general assumption for each slickenside data: $B_i \cdot T \cdot N_i = 0$. Using the slip vector $SV_i = [SV_X \ SV_Y \ SV_Z]$ and the plane normal vector $N_i = [N_X \ N_Y \ N_Z]$, we can have the following equations:

$$B_i \cdot T \cdot N_i = [b_1 \ b_2 \ b_3] \cdot \begin{bmatrix} \sigma_{11} & \sigma_{12} & \sigma_{13} \\ \sigma_{12} & \sigma_{22} & \sigma_{23} \\ \sigma_{13} & \sigma_{23} & \sigma_{33} \end{bmatrix} \cdot \begin{bmatrix} N_X \\ N_Y \\ N_Z \end{bmatrix} = 0$$

or in algebraic format

$$\begin{aligned} & b_1 \sigma_{11} N_X + b_1 \sigma_{12} N_Y + b_1 \sigma_{13} N_Z + \\ & b_2 \sigma_{12} N_X + b_2 \sigma_{22} N_Y + b_2 \sigma_{23} N_Z + \\ & b_3 \sigma_{13} N_X + b_3 \sigma_{23} N_Y + b_3 \sigma_{33} N_Z = 0 \end{aligned}$$

where

$$B_i = SV_i \otimes N_i = [b_1 \quad b_2 \quad b_3], \text{ and}$$

$$T = \begin{bmatrix} \sigma_{11} & \sigma_{12} & \sigma_{13} \\ \sigma_{12} & \sigma_{22} & \sigma_{23} \\ \sigma_{13} & \sigma_{23} & \sigma_{33} \end{bmatrix};$$

- Use regression to search for the best fitting values of T : calculate the P sum of the inner products of p_i vectors:

$$P = \sum_{i=1}^n p_i \cdot p_i^T$$

where

$$p_i = [b_1 n_{i1} \quad b_2 n_{i2} \quad b_3 n_{i3} \quad b_1 n_{i2} + b_2 n_{i1} \quad b_2 n_{i3} + b_3 n_{i2} \quad b_1 n_{i3} + b_3 n_{i1}];$$

- Find the eigenvalues and eigenvectors of the P matrix, choose the second smallest eigenvalue's referring eigenvector E and use it to express T stress tensor:

$$T = \begin{bmatrix} \sigma_{11} & \sigma_{12} & \sigma_{13} \\ \sigma_{12} & \sigma_{22} & \sigma_{23} \\ \sigma_{13} & \sigma_{23} & \sigma_{33} \end{bmatrix} = \begin{bmatrix} E_1 & E_4 & E_6 \\ E_4 & E_2 & E_5 \\ E_6 & E_5 & E_3 \end{bmatrix}$$

where

$$E = [E_1 \quad E_2 \quad E_3 \quad E_4 \quad E_5 \quad E_6].$$

This methodology is really similar to Fry's (1999) solution; the most important difference is the reduction in the dimensions number using Angelier's (1979) assumption: $\sigma_{11} + \sigma_{22} + \sigma_{33} = 0$.

- Vector p_i (used in Fry's 1999 methodology) will have the following form:

$$p_i = [b_1 n_1 - b_3 n_3 \quad b_2 n_2 - b_3 n_3 \quad b_1 n_2 + b_2 n_1 \quad b_1 n_3 + b_3 n_1 \quad b_2 n_3 + b_3 n_2]$$

- Apply Fry's (1999) procedure to find the eigenvalues and eigenvectors of the P matrix, and choose referring eigenvector E of the smallest eigenvalue to calculate T stress tensor:

$$T = \begin{bmatrix} \sigma_{11} & \sigma_{12} & \sigma_{13} \\ \sigma_{12} & \sigma_{22} & \sigma_{23} \\ \sigma_{13} & \sigma_{23} & \sigma_{33} \end{bmatrix} = \begin{bmatrix} E_1 & E_3 & E_4 \\ E_3 & E_2 & E_5 \\ E_4 & E_5 & 0 - E_1 - E_2 \end{bmatrix},$$

where

$$E = [E_1 \quad E_2 \quad E_3 \quad E_4 \quad E_5].$$

1F MICHAEL (1984)

Michael's (1984) methodology uses the relationship between the stress tensor T , the (resolved) shear stress vector τ_i and the plane normal vector ($N_i = [N_X \ N_Y \ N_Z]$) for the i^{th} slickenside. In this case $\tau_i = [\tau_X \ \tau_Y \ \tau_Z] = T N_i - ((T N_i) \otimes N_i) N_i$. Assuming the observed slip vector ($SV_i = [SV_X \ SV_Y \ SV_Z]$) equals to the resolved shear vector τ_i , and supposing $\sigma_{11} + \sigma_{22} + \sigma_{33} = 0$ after Angelier (1979), we have the matrix equation $M_i X = SV_i$, where

$$M_i = \begin{bmatrix} n_1 - n_1^3 + n_1 n_3^2 & n_2 - 2n_2 n_1^2 & n_3 - 2n_3 n_1^2 & -n_1 n_2^2 + n_1 n_3^2 & -2n_1 n_2 n_3 \\ -n_2 n_1^2 + n_2 n_3^2 & n_1 - 2n_1 n_2^2 & -2n_1 n_2 n_3 & n_2 - n_2^3 + n_2 n_3^2 & n_3 - 2n_3 n_2^2 \\ -n_3 n_1^2 - n_3 + n_3^3 & -2n_1 n_2 n_3 & n_1 - 2n_1 n_3^2 & -n_2^2 n_3 - n_3 + n_3^3 & n_2 - 2n_2 n_3^2 \end{bmatrix},$$

and

$$X = [\sigma_{11} \quad \sigma_{12} \quad \sigma_{13} \quad \sigma_{22} \quad \sigma_{23}].$$

- Calculate the following and M and SV hypermatrices and solve the linear equation system to get X .

$$M = \begin{bmatrix} M_1^T \\ \vdots \\ M_i^T \\ \vdots \\ M_n^T \end{bmatrix}, \text{ and } SV = \begin{bmatrix} SV_1^T \\ \vdots \\ SV_i^T \\ \vdots \\ SV_n^T \end{bmatrix}$$

1G ANGELIER (1990)

This methodology calculates the misfit vector v_i between the measured slip vector $SV_i = [SV_X \quad SV_Y \quad SV_Z]$ and resolved shear stress vector $\tau_i = [\tau_X \quad \tau_Y \quad \tau_Z]$. After [Angelier \(1979\)](#) we can assume $\sigma_{11} + \sigma_{22} + \sigma_{33} = 0$ and $\sigma_{11}^2 + \sigma_{22}^2 + \sigma_{33}^2 = 3/2$; stress tensor T will have the following well known form:

$$T = \begin{bmatrix} \sigma_{11} & \sigma_{12} & \sigma_{13} \\ \sigma_{12} & \sigma_{22} & \sigma_{23} \\ \sigma_{13} & \sigma_{23} & \sigma_{33} \end{bmatrix} = \begin{bmatrix} \cos(\psi) & \alpha & \gamma \\ \alpha & \cos\left(\psi + \frac{2\pi}{3}\right) & \beta \\ \gamma & \beta & \cos\left(\psi + \frac{4\pi}{3}\right) \end{bmatrix}$$

- Length of vector v_i is expressed as a function of the N_i , SV_i , the assumed shear stress vector length λ_i and the four unknown members of stress tensor (α , β , γ and ψ). To minimize the length of v_i vector, the following partial derivatives are calculated:

$$\frac{1}{2} \frac{\partial v^2}{\partial \alpha} = 0, \quad \frac{1}{2} \frac{\partial v^2}{\partial \beta} = 0, \quad \frac{1}{2} \frac{\partial v^2}{\partial \gamma} = 0, \quad \text{and} \quad \frac{1}{2} \frac{\partial v^2}{\partial \psi} = 0$$

- The final equation (A15 in [Angelier 1990](#)) is the function of ψ on the fourth power, usually, has two real (ψ_1 and ψ_2) and two complex solutions;
- Calculate α , β and γ values using both ψ_1 and ψ_2 , and choose the best fitting stress tensor.

1H MOSTAFA (2005)

Using [Angelier's \(1990\)](#) methodology, [Mostafa \(2005\)](#) proposed the following iterative loop to find the ideal shear vector length λ_i :

- assume the initial shear vector length λ_i equals to $\sqrt{3/2}$,
- calculate the stress tensor using [Angelier's \(1990\)](#) methodology,
- calculate the resolved shear vector (τ_i) length,
- use $\lambda_i = \tau_i$ in the following iteration steps until reaching any user defined convergence criteria; according to the practical experience, no significant change after the 15th - 20th loop is noticed.

REFERENCES

- Adobe Developer Support, 1992. Encapsulated PostScript – File Format Specification, Version 3.0, Tech Note #5002, Adobe Systems Incorporated, San Jose, CA, USA, 34pp.
http://partners.adobe.com/public/developer/en/ps/5002.EPSF_Spec.pdf
[Accessed April 30, 2013].
- Adobe Systems Incorporated, 2006. PDF reference: Adobe Portable Document Format, Version 1.7, 1310pp
http://wwwimages.adobe.com/www.adobe.com/content/dam/Adobe/en/devnet/pdf/pdfs/pdf_reference_1-7.pdf [Accessed April 30, 2013].
- Anderson, E.M., 1942. Dynamics of faulting and dyke formation with applications to Britain, 1st edn., Oliver and Boyd, Edinburgh, 206pp.

- Angelier, J., 1975. Sur l'analyse de mesures recueillies dans des sites failles: l'utilite d'une confrontation entre les methods dynamiques et cinematiques. Comptes Rendus des Seances de l' Academic des Sciences Paris D 281, 1805-1808.
- Angelier, J., 1979. Determination of the mean principal directions of stresses for a given fault population. Tectonophysics 56(3-4), T17-T26.
- Angelier, J., 1984. Tectonic analysis of fault slip data sets. Journal of Geophysical Research 89(B7), 5835-5848.
- Angelier, J., 1990. Inversion of field data in fault tectonics to obtain the regional stress III: A new rapid direct inversion method by analytical means. Geophysical Journal International 103(2), 363-376.
- Angelier, J., Goguel, J., 1979. Sur une méthode simple de détermination des axes principaux des contraintes pour une population de failles. Comptes Rendus Hebdomadaires des Séances de l'Academie des Sciences 288(1), 307-310.
- Angelier, J., Mechler, P., 1977. Sur une méthode graphique de recherche des contraintes principales également utilisable en tectonique et en séismologie: la methode des dièdres droits. Bulletin de la Société Géologique de France 7, 19(6), 1309-1318.
- Bingham, C., 1964. Distributions on the sphere and on the projective plane. PhD Dissertation, Yale University, New Haven, United States of America, 80pp.
- Bingham, C., 1974. An antipodally symmetric distribution on the sphere. Annales of Statistics 2(6), 1201-1225.

- Bishop, A.W., 1966. The strength of soils as engineering materials. *Géotechnique* 16(2), 91-128.
- Cardozo, N., Allmendinger, R.W., 2013. Spherical projections with OSXStereonet. *Computers & Geosciences* 51, 193-205.
- Carey, M.E., Brunier, M.B., 1974. Analyse théorique et numérique d'une modèle mécanique élémentaire applique a l'étude d'une population de failles. *Comptes Rendus Hebdomadaires des Séances de l'Academie des Sciences* 279D, 891-894.
- Delvaux, D., Sperner, B., 2003. New aspects of tectonic stress inversion with reference to the TENSOR program, In: Nieuwland, D., (Ed.) *New insights into structural interpretation and modelling*, Geological Society, London, Special Publications, Vol. 212, pp. 75-100.
- Delvaux, D., Moeys, R., Stapel, G., Petit, C., Levi, K., Miroshnichenko, A., Ruzhich, V., Sankov, V., 1997. Paleostress reconstructions and geodynamics of the Baikal region, Central Asia. Part II: Cenozoic rifting. *Tectonophysics* 282(1-4), 1-38.
- Dips 6.0, 2013.
<https://www.rocscience.com/products/1/Dips?gclid=CP3Olrus7LYCFcmz3god0EoAfQ> [Accessed April 28, 2013].
- Etchecopar, A., Vasseur, G., Daignieres, M. 1981. An inverse problem in microtectonics for the determination of stress tensors from fault striation analysis. *Journal of Structural Geology* 3(1), 51-65.
- Fabric 8, 2012. <http://www.geolsoft.com/index.html> [Accessed April 29, 2013].

- Faille 4.3, 2010: http://www.pages-perso-bernard-celierier.univ-montp2.fr/software/bin/Windows_XP/faille/faille_4.3_winxp.zip [Accessed April 30, 2013].
- FaultKin 6, 2013: <http://www.geo.cornell.edu/geology/faculty/RWA/programs/faultkin.html> [Accessed April 28, 2013].
- Fry, N., 1999. Striated faults: visual appreciation of their constraint on possible palaeostress tensors. *Journal of Structural Geology* 21(1), 7-27.
- FSA 34.5, 2013. <http://www.pages-perso-bernard-celierier.univ-montp2.fr/software/dcm/gra/softw.wind.html> [Accessed April 29, 2013].
- GEOrient 9, 2011. http://www.holcombe.net.au/software/rodh_software_georient.htm [Accessed April 28, 2013].
- Gephart, J.W., 1990. Stress and the direction of slip on fault planes. *Tectonics* 9(4), 845-858.
- Gephart, J.W., Forsyth, D.W. 1984. An improved method for determining the regional stress tensor using earthquake focal mechanism data: Application to the San Fernando Earthquake sequence, *Journal of Geophysical Research* 89(B11), 9305-9320.
- Handin, J. 1966. Strength and ductility, In: Clark, S. P., Jr. (Ed.) *Handbook of Physical Constants – Revised Edition*. Geological Society of America Memoires 97, pp. 223-289.
- Hardcastle, K.C., Hills, L.S. 1991. Brute3 and Select: QuickBasic 4 program for determination of stress tensor configurations and separation of

- heterogeneous populations of fault slip data. *Computers & Geosciences* 17(1), 23-43.
- Hoepfner, R., 1955. Tektonik im Schiefergebirge. *Geologische Rundschau* 44(1), 26-58.
 - Huang, Q., 1988. Computer-based method to separate heterogeneous sets of fault-slip data into subsets. *Journal of Structural Geology* 10(3), 278-299.
 - Krejci, D., Richter, C., 1991. SPLIT: a Turbo-C program for the graphical representation and separation of fault-slip data sets. *Computers & Geosciences* 17(6), 801-811.
 - Lisle, R.J., 1988. ROMSA: A BASIC program for paleostress analysis using fault-striation data. *Computers & Geosciences* 14(2), 255-259.
 - Lisle, R.J., Orife, T., 2002. STRESSTAT: A Basic program for numerical evaluation of stress inversion results. *Computers & Geosciences* 28(9), 1037-1040.
 - MacQueen, J.B., 1967. Some Methods for classification and analysis of multivariate observations. In: *Proceedings of 5th Berkeley Symposium on Mathematical Statistics and Probability*, University of California Press 1, 281-297.
 - Michael, A., 1984. Determination of stress from slip data: fault and folds, *Journal of Geophysical Research* 89B, 11517-11526.
 - Mostafa, M.E., 2005. Iterative direct inversion: An exact complementary solution for inverting fault-slip data to obtain palaeostresses. *Computers & Geosciences* 31(8), 1059-1070.
 - MyFault, 2013. <http://pangaeasci.com/index.php?page=myfault> [Accessed March 03, 2013].

- Nemčok, M., Lisle, R.J., 1995. A stress inversion procedure for polyphase fault/slip data sets. *Journal of Structural Geology* 17(10), 1445-1453.
- Nemčok, M., Kovač, D., Lisle, R.J., 1999. Stress inversion procedure for polyphase calcite twin and fault/slip data sets. *Journal of Structural Geology* 21(6), 597-611.
- Openstereo, 2011. <http://www.igc.usp.br/index.php?id=395> [Accessed April 28, 2013].
- Orient, 2012. <http://www.frederickvollmer.com/orient/> [Accessed April 17, 2013].
- Orife, T., Arlegui, L., Lisle, R.J., 2002. DIPSLIP: A QuickBasic stress inversion program for analysing sets of faults without slip lineations. *Computers & Geosciences* 28(6), 775-781.
- Ortner, H., Reiter, F., Acs, P., 2002. Easy handling of tectonic data: the programs TectonicVB for Mac and TectonicsFP for Windows. *Computers & Geosciences* 28(10), 1193-1200.
- OSXStereonet For Mac 1.7, 2012. http://www.downloadplex.com/Mac/Education/Other/osxstereonet-for-mac_365379.html [Accessed April 28, 2013].
- Pascal, C., 2004. SORTAN: a Unix program for calculation and graphical presentation of fault slip as induced by stresses. *Computers & Geosciences* 30(3), 259-265.
- Reches, Z., 1987. Determination of the tectonic stress tensor from slip along faults with Coulomb yield condition. *Tectonics* 6(6), 849-861.

- RockWare SpheriStat 3.2, 2013:
<http://www.rockware.com/product/overview.php?id=127> [Accessed April 28, 2013].
- RockWare StereoStat 1.6, 2013:
<http://www.rockware.com/product/overview.php?id=121> [Accessed April 28, 2013].
- Shafranovich, Y., 2005. Common Format and MIME Type for Comma-Separated Values (CSV) Files. SolidMatrix Technologies, Inc., 8pp.
<http://tools.ietf.org/html/rfc4180> [Accessed April 30, 2013].
- Shan, Y., Li, Z., Lin, G., 2004. A stress inversion procedure for automatic recognition of polyphase fault/slip data sets. *Journal of Structural Geology* 26(5), 919-925.
- Shorrock, C., Lisle, R.J., 1998. DATACON: A QuickBasic program to reformat orientation data from faults. *Computers & Geosciences* 24(6), 585-590.
- Sperner, B., Ratschbacher, L., 1994. A Turbo Pascal program package for graphical representation and stress analysis of calcite deformation. *Zeitschrift Deutsche Geologische Gesellschaft* 145, 414-423.
- Sperner, B., Ratschbacher, L., Ott, R., 1993. Fault striae analysis: a Turbo Pascal program package for graphical presentation and reduced stress tensor calculation. *Computers & Geosciences* 19(9), 1362-1388.
- Spang, J.H., 1972. Numerical method for dynamic analysis of calcite twin lamellae. *Geological Society of America Bulletin* 83(2), 467-472.
- Steinhaus, H., 1957, Sur la division des corps matériels en parties. *Bulletin de l'Académie Polonaise des Sciences, Classe 3*, 4(12), 801-804 (in French).

- Stereonet 8, 2013.
<http://www.geo.cornell.edu/geology/faculty/RWA/programs/stereonet.html>
[Accessed April 28, 2013].
- Stereonet Web Application (no development information):
<http://app.visiblegeology.com/stereonetApp.html> [Accessed April 28, 2013].
- Taboada, A., Tournieret, C., Laurent, P., 1991. An interactive program for the graphical representation of striated faults and applied normal and tangential stresses. *Computers and Geosciences* 17(9), 1281-1310.
- TECTOR, 1994. <https://sites.google.com/site/jacquesangelier/webcounter>
[Accessed March 03, 2013].
- TECTOR, 2000. <https://sites.google.com/site/jacquesangelier/structuresacceptedintectorsoftwares> [Accessed March 03, 2013].
- Tobore, O., Lisle, R.J., 2003. Numerical processing of palaeostress results. *Journal of Structural Geology* 25(6), 949-957.
- Tomita, S., Yamaji, A., 2004. KUT: Software to rotate orientation data. *Geoinformatics* 14(2), 85-104 (in Japanese with English abstract).
- Turner, F.J., 1953. Nature and dynamic interpretation of deformation lamellae in calcite of three marbles. *American Journal of Science* 251, 276-298.
- Will, T.M., Powell, R., 1991. A robust approach to the calculation of paleostress fields from fault plane data. *Journal of Structural Geology* 13(7), 813-821.
- Win-Tensor 4.0, 2012. <http://www.damiendelvaux.be/Tensor/tensor-index.html> [Accessed March 04, 2013].

- Yamaji, A., 2000. The multiple inverse method: A new technique to separate stresses from heterogeneous fault-slip data. *Journal of Structural Geology* 22(4), 441-452.
- Yamaji, A. 2001. A stereonet program for fault-striation analysis. *Geoinformatics* 12(3), 167-182 (in Japanese with English abstract).
- Yin, Z.M., Ranalli, G., 1995. Estimation of the frictional strength of faults from inversion of fault-slip data - a new method. *Journal of Structural Geology* 17(9), 1327-1335.
- Žalohar, J., Vrabec, M., 2007. Paleostress analysis of heterogeneous fault-slip data: the Gauss method. *Journal of Structural Geology* 29(11), 1798-1810.

FIGURE AND TABLE CAPTIONS

- Figure 1: Screenshot of graphical user interface. A) File operation menu bar, B) Project status bar, C) Settings panel, D) Run button, E) Encapsulated PostScript to portable document format conversion status bar.
- Figure 2: Result plot with stereograophical projections and rose plots. Stereonets and rose diagrams for A) observed and B) BN rotated data; C) Data locality, data type and group name; D) Number of displayed data with the average bedding and BN rotation methodology; E) Plot type, projection and hemisphere; F) Paleostress inversion or weight point calculation result; G) Maximum, intermediate and minimum stress directions or weight axis orientation; H) Stress regime after [Delvaux et al. \(1997\)](#); I) RUP (relative upslon) bar after [Angelier \(1990\)](#); J) ANG bar (angular misfit) bar after [Angelier \(1990\)](#); K) Main circular rose diagram for strike or dip direction

distribution; L) Small quadrant plot for vertical (dip angle or plunge) directional statistics; M) Mohr circle to show stress status.

- Figure 3: Stereographical projection of the same data set plotted using A) equal area and B) equal angle projection (data set with equal area projection in light gray as background for comparison). TYM dataset of [Angelier \(1990\)](#).
- Figure 4: BN rotation results. A) Original TYM dataset of [Angelier \(1990\)](#), B) Original data set rotated to correct 050/80 average bedding (dip direction convention used), C) Original data set rotated by +30 degrees paleomagnetic declinations for each data, D) Original data set rotated to correct 050/80 average bedding and rotated by +30 degrees paleomagnetic declinations.
- Figure 5: Using groups during data sets evaluation. A) Data set with three user defined groups are processed *using groups processing option*: all of three data groups defined in input file will be processed and displayed one by one. B) Same data set *not using groups processing option*: all data will be processed altogether and displayed using different colours (different line styles are used on the grayscale figure).
- Figure 6: Clustering result for the same data set (A) using two (B), three (C), four (D), five (E) and six (F) clusters.
- Figure 7: Comparison of the result using different stress field calculation methodologies for [Angelier's \(1990\)](#) AVB data set. A) PTN after [Turner \(1953\)](#) with $\alpha = 30$ degrees, B) NDA after [Spang \(1972\)](#) with $\alpha = 30$ degrees, C) after [Fry \(1999\)](#), D) after [Shan et al. \(2004\)](#), E) after [Michael \(1984\)](#) regression methodologies, F) after [Angelier \(1990\)](#) and G) [Mostafa's \(2005\)](#) methodology. Please note changes in stress field characteristics indicated by Mohr-circles; please note change in RUP and ANG stress estimators

distribution in the case of [Mostafa's \(2005\)](#) paleostress inversion relative to [Angelier's \(1990\)](#) methodology.

- Figure 8: Data set processed A) without and B) with virtual symmetric data set option. Please note change in stress axes direction and in reduced stress tensor.
- Figure 9: Same fracture data set plotted on asymmetrical and symmetrical rose diagrams. A) Asymmetrical plot with 2.5 degrees bin size, B) Asymmetrical plot with 22.5 degrees bin size, C) Symmetrical plot with 2.5 degrees bin size, D) Symmetrical plot with 22.5 degrees bin size. Same data
- Table 1: Comparison chart for selected computer based implementations and web applications for field data processing.



A

Project: **ang2**, path: C:\Personal\sg2ps_gui

Data file found

Settings from a previous run found

Not using any coordinate file

B

Settings

Data convention German dip direction

Plot type Angelier plot

Projection type Schmidt

Hemisphere Lower

Bedding & palaeonorth correction Both

Sort by groups as well No

Cluster numbers Don't use

Labelling No

Inversion methodology Michael (1984)

Virtual symmetrical data set No

Ideal movement direction display Yes

Maximum stress & slickenside direction angle 30

Fracture weight point statistics Bingham statistics

Line width used on stereonet in points 0.6

Type of the rose plot Symmetric

Bin size for rose plot in degrees 10.0

C

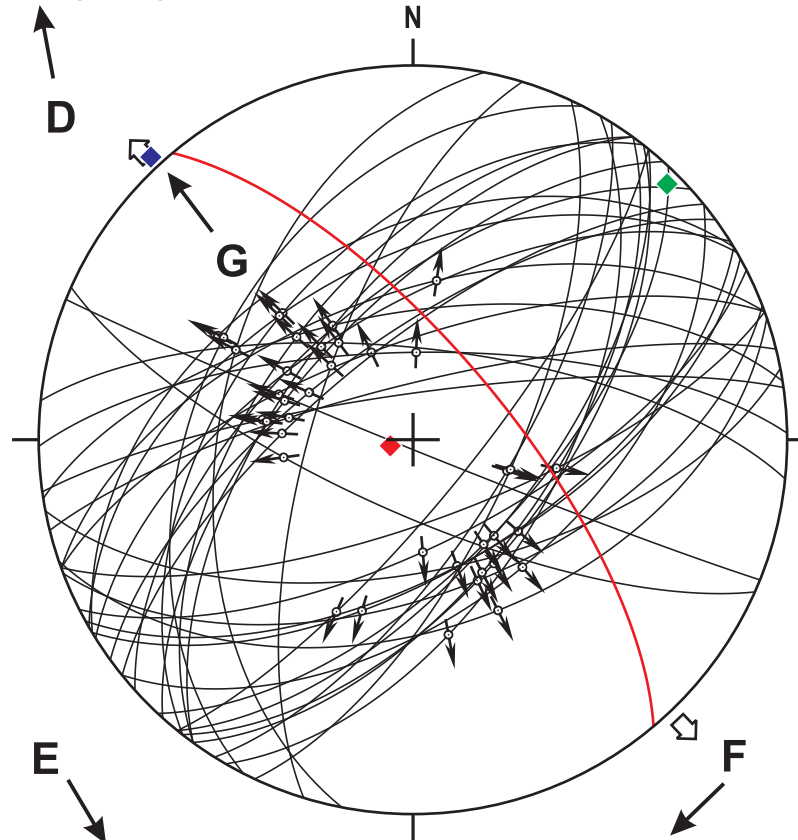
Run

D

E

ALL OBSERVED STRIAE DATA FROM DATA POINT ANG002

Data number: 38
Average bedding: 050/70

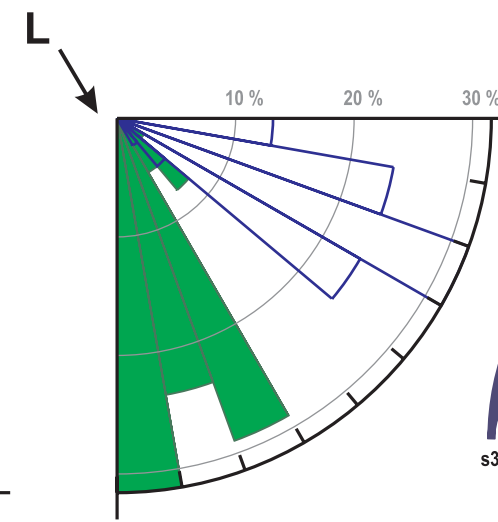
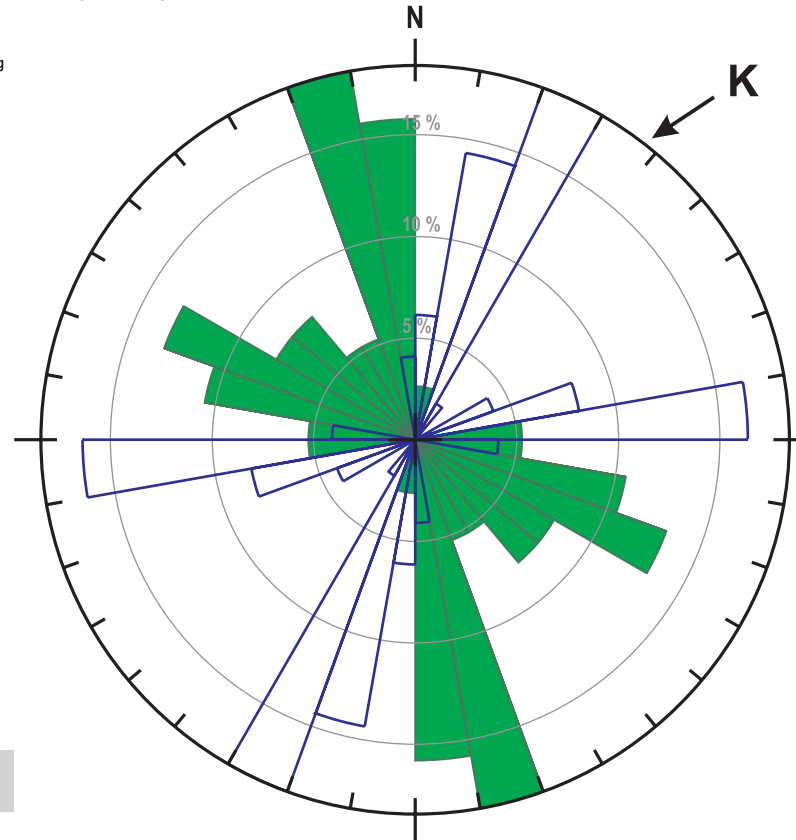


Angelier-plot, Schmidt-net, lower hemisphere

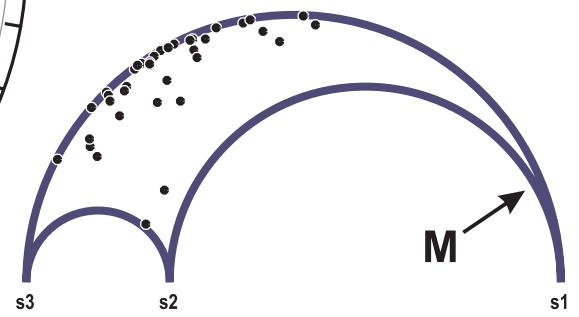
Inversion after Angelier (1990)
S1: 226/85, S2: 047/05, S3: 317/00
R: 0.268, R': 0.268, PURE EXTENSIVE



Rose plot for measured data
Average bedding: 050/70



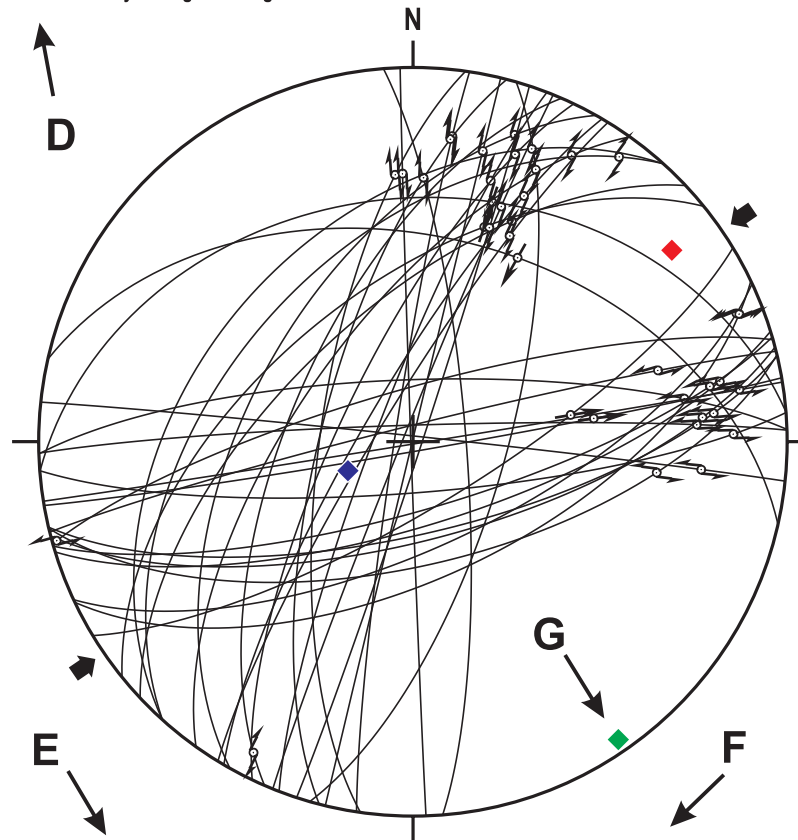
ORIGINAL



SYMBOLS

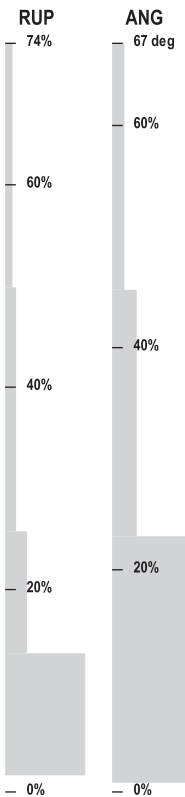
FAULT AND STRIAE DATA	STRESS INVERSION	ROSE PLOT	GROUPS
Fault plane Group 'X'	S1 axis (red diamond)	Plane dip direction (green wedge)	Group 'A' (blue line)
Average bedding (red arc)	S2 axis (green diamond)	Lineation dip direction (blue wedge)	Group 'B' (pink line)
Average bedding Overturned (red dotted arc)	S3 axis (blue diamond)		Group 'C' (red line)
Normal fault (arrow pointing away)	Maximum horizontal stress (black arrow)		Group 'D' (orange line)
Reverse fault (arrow pointing towards)	Minimum horizontal stress (white arrow)		Group 'E' (yellow line)
Dextral fault (arrow pointing right)			Group 'F' (green line)
Sinistral fault (arrow pointing left)			Group 'G' (pink line)
Unknown fault (arrow pointing up)			Group 'H' (blue line)
Ideal movement (arrow pointing down)			Group 'I' (grey line)

Data number: 38
Corrected by average bedding 050/70

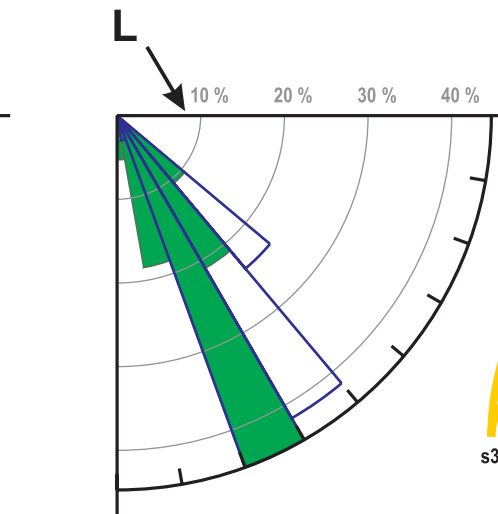
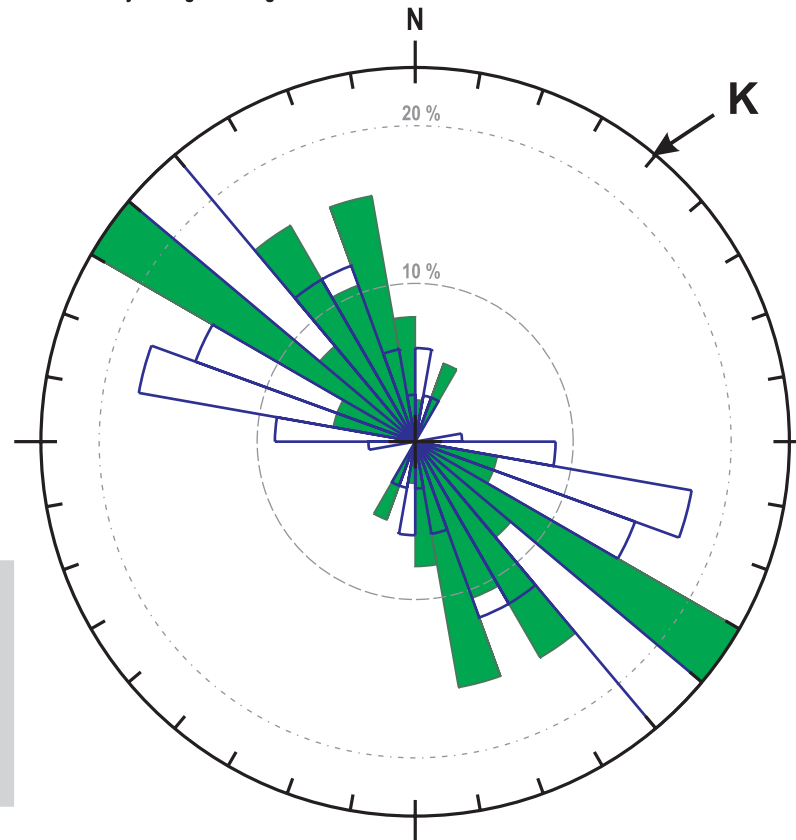


Angelier-plot, Schmidt-net, lower hemisphere

Inversion after Angelier (1990)
S1: 056/16, S2: 146/00, S3: 236/74
R: 0.193, R': 2.193, TRANSPRESSIVE



Rose plot for dip corrected data
Corrected by average bedding 050/70



CORRECTED

